tvst

https://doi.org/10.1167/tvst.8.6.47

Article

Topical Trabodenoson Is Neuroprotective in a Rodent Model of Anterior Ischemic Optic Neuropathy (rNAION)

Yan Guo[1], Zara Mehrabian[1], Mary A. Johnson[1], David S. Albers[2], Cadmus C. Rich[3], Rudolf A. Baumgartner[4], and Steven L. Bernstein[1]

[1] Department of Ophthalmology and Visual Sciences, University of Maryland at Baltimore-School of Medicine, Baltimore, MD, USA
[2] ReNeuron, Inc., Burlington, MA, USA
[3] Aura Biosciences, Inc., Cambridge, MA, USA
[4] Flatley Discovery Lab, LLC, Charlestown, MA, USA

Correspondence: Steven L. Bernstein, MSTF 5-00B, 10 South Pine Street, Baltimore, MD 21201, USA. e-mail: sbernstein@som.umaryland.edu

Received: 5 March 2019
Accepted: 20 October 2019
Published: 20 December 2019

Keywords: nonarteritic anterior ischemic optic neuropathy (NAION); optic nerve; ischemia; adenosine receptor mimetics; edema; neuroprotection; astrocytes

Citation: Guo Y, Mehrabian Z, Johnson MA, Albers DS, Rich CC, Baumgartner RA, Bernstein SL. Topical trabodenoson is neuroprotective in a rodent model of anterior ischemic optic neuropathy (rNAION). Trans Vis Sci Tech. 2019;8(6):47, https://doi.org/10.1167/tvst.8.6.47

Purpose: Nonarteritic anterior ischemic optic neuropathy (NAION) is the leading cause of sudden optic nerve–related vision loss currently without effective treatment. We evaluated the neuroprotective potential of ocular (topical) delivery of trabodenoson, a selective A_1 receptor mimetic, in a rodent model of NAION (rNAION).

Methods: Daily topical delivery of 3% trabodenoson or vehicle administered in both eyes 3 days prior to rNAION induction and for 21 days post induction. Retinal appearance and optic nerve head (ONH) edema was evaluated using spectral-domain optical coherence tomography (SD-OCT). Retinal function was evaluated before and after induction by ganzfeld electroretinography (ERG). Brn3a(+) retinal ganglion cells (RGCs) were quantified by stereology. Axonal ultrastructure was evaluated by electron microscopy.

Results: Trabodenoson-treated eyes had significantly reduced optic nerve (ON) edema compared with vehicle-treated eyes (ANOVA, $P < 0.05$). Electrophysiologically, there was a nonsignificant trend toward b-wave and oscillatory potential (OP) preservation in the trabodenoson-treated eyes. RGC counts were higher in trabodenoson-treated eyes compared to vehicle (74% versus 47% of the contralateral eye; two-tailed *t*-test; $P = 0.01$), as were ON axons. No overt morphologic differences in cell inflammation were observed between vehicle- and trabodenoson-treated ONHs, but trabodenoson-treated ONHs revealed increased expression of astrocyte-related neuroprotective responses.

Conclusions: Trabodenoson preserves RGCs in the rodent NAION model. While previous clinical trials focused on trabodenoson's ocular antihypertensive effect, our data suggest trabodenoson's primary target may be both the retina and ONH. Selective adenosine A_1 agonists may prove an appropriate neuroprotective adjunctive for ischemia-related ON diseases such as NAION and glaucoma.

Translational Relevance: RGC and ON neuroprotection in ischemic neuropathies may be achievable by topical administration of A_1 adenosine agonists rather than by simply relying on intraocular pressure reduction.

Introduction

Nonarteritic anterior ischemic optic neuropathy (NAION) is the leading cause of sudden optic nerve (ON)-related vision loss in individuals 50 years or older in the United States.[1] NAION is caused by ischemia at the optic nerve head (ONH), with resulting edema and development of a compartment syndrome, leading to progressive axonal damage and retinal ganglion cell (RGC) loss. NAION's pathophysiology remains poorly understood and no effective treatment is currently available. Animal models of NAION have been developed that recapitulate many of the pathophysiological aspects of the natural disease, exhibiting many of the structural, histologic,

and functional deficits observed in the human condition.[2] These models have proved useful in evaluating neuroprotective strategies.

Adenosine can exert both neuroprotective and neurodegenerative actions; these effects are mediated through a variety of adenosine receptors. While activation of the A_1 receptor (A_1R) is largely neuroprotective,[3–5] A_2R stimulation can be either neurodegenerative or neuroprotective, depending on the models and timing.[6,7] Intraretinally, evidence for A_1R's neuroprotective role comes from studies showing the benefits of ischemic preconditioning against subsequent ischemic events that otherwise result in cellular damage.[8] However, multiple A_1R neuroprotective mechanisms have been demonstrated, including astrocyte and inflammatory modulation[5,9,10] and neural stem cell proliferation.[11] Astrocyte reactivity and inflammation are important components in anterior ON ischemic disease and glaucoma.[12–14]

Trabodenoson is a highly selective lipophilic, potent A_1R mimetic initially developed clinically for primary open-angle glaucoma (OAG) because it was previously shown to lower intraocular pressure (IOP) by increasing conventional outflow facility.[15,16] Delivered as a topical (ocular) drop, 3% trabodenoson can achieve intraretinal and ON concentrations exceeding the affinity constant (Ki) for A_1R (0.97 nmol), lasting for up to 8 hours post administration in several preclinical species.[17] We wanted to determine whether A_1R stimulation might be directly RGC neuroprotective in diseases such as NAION without the requirement of IOP modification. Thus, we evaluated topical trabodenoson effects on RGC survival and ON function in the rat model of NAION (rNAION). We chose expression markers associated with both the ischemic preconditioning neuroprotective response, such as heme oxygenase-1 (Hmox1),[18,19] astrocyte neuroprotection responses such as nestin,[20,21] astrocyte damage responses (glial fibrillary acidic protein [GFAP]) and matrix metalloproteinase-2 (mmp2),[22–24] and an additional neuroprogenitor-associated gene, *Sox2*.[25] Thy-1 was used as a gross marker for RGC loss.[26] Because of the limited number of samples used for each analysis (eight per group, including replicates), we set the significance level at $P < 0.01$ rather than the more typical $P < 0.05$.

Material and Methods

Animals

Animal protocols were approved by the University of Maryland-Baltimore Institutional Animal Care and Use Committee (IACUC), and animals were handled in accordance with the ARVO Statement for the Use of Animals in Ophthalmic and Vision Research. Male Sprague-Dawley rats (200–300 g) were obtained from Harlan Labs (Indianapolis, IN) and kept in an accredited animal facility with food and water available ad libitum. Animals were grouped into short-term treatment animals (2 days post rNAION induction analysis; $n = 2$ eyes/group for immunohistochemistry and $n = 8$ eyes/group for gene expression analysis). Long-term treatment animals (30 days post rNAION; $n = 13$ animals/group; total of 26 animals), were used for RGC stereology. All animals held by glove received either twice daily ocular drops of 3% trabodenoson or vehicle in both eyes starting 3 days prior to rNAION induction. Long-term treatment animals received drops every day post rNAION for 21 days post induction. There were no indications of any discomfort upon or after topical drop administration of either trabodenoson or vehicle. Animals were anesthetized with 1 mL/kg intraperitoneal 80 mg/mL ketamine-4 mg/mL xylazine for rNAION induction and all other testing procedures.

rNAION Induction and Visualization

As previously described,[27] rNAION was unilaterally induced using a fundus contact lens, intravenous injection with rose Bengal dye, and 11 seconds of unilateral intraocular ON laser illumination using a 532-nm frequency-doubled ND-YAG laser (Iridex Corp., Mountain View, CA). Each animal's contralateral eye served as the control eye.

Optical Coherence Tomography (OCT) of the Retina and ON

Ocular fundi were imaged in vivo 2 days post induction using spectral-domain OCT (SD-OCT; Heidelberg Engineering, Heidelberg, Germany), incorporating the commercially available rodent eye-correcting 28-diopter lens and a plano-concave contact lens, enabling in vivo cross-sectional analysis of the retinal layers and ON to the depth of the choroid and lamina, respectively. The identity of each eye (vehicle, trabodenoson) was masked to the investigator analyzing the nerve edema, and the extent of edema in the intraocular portion of the ON was quantified using the tool available in the Heidelberg device by measuring the diameter of the nerve fibers spanning the visible edges of the inner nuclear layer (INL) on either side of the nerve space (white lines above retina, Fig. 1B, D, F).

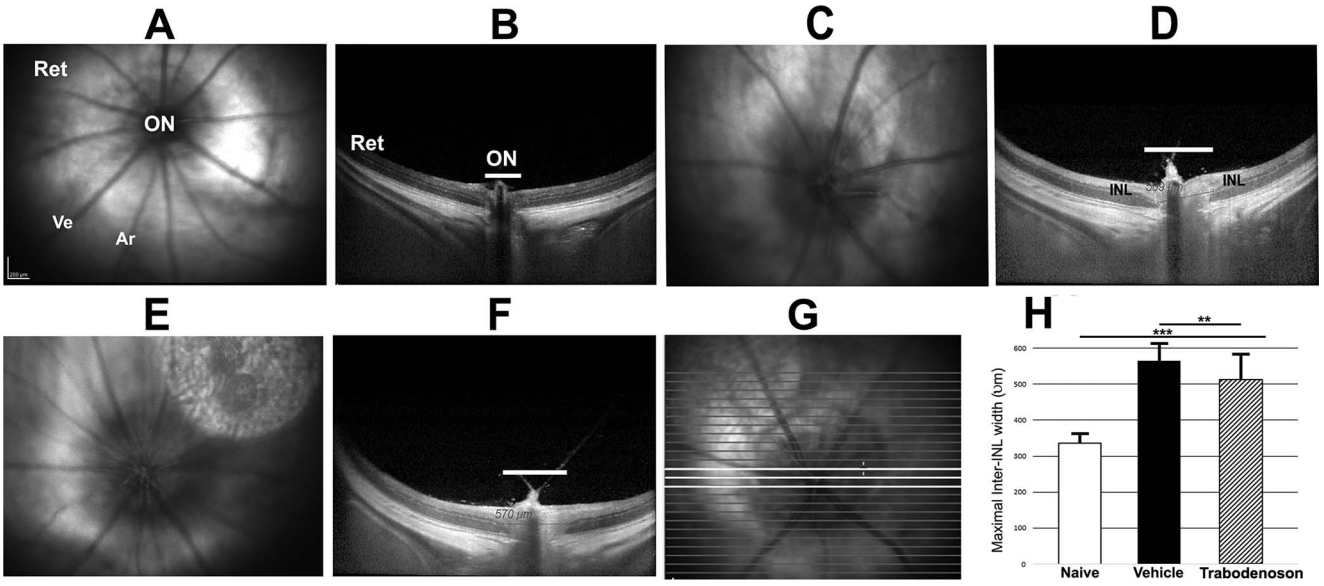

Figure 1. SD-OCT en face (A, C, E) and cross-sectional (B, D, F) analysis of the retina (Ret) and intraocular ON. In (A, B) naïve (noninduced) eye; (C, D) induced eye treated with vehicle eyedrops; (E, F) induced eye treated with trabodenoson eyedrops. The *white bar* indicates the intraretinal space between the inner nuclear layers (INLs) on either side of the ON. (A) Naïve eye is labeled to show retina (Ret) and ON. There is no ON edema, and the ON image appears flat against the retina. (B) Naïve eye, cross section. The inter-INL gap is shown at the maximal width (*white bar*). (C) Vehicle-treated eye/induced. ON edema is apparent in the en face view. (D) Cross section: The inter-INL gap has widened, indicating edema. (E) Trabodenoson-treated eye/induced. ON edema is apparent. (F) Cross section: the INL-INL gap is shown in *white* and reported by the tool available from the SD-OCT instrument. (G) Analysis of mean maximal ON edema. The ON region of the fundus was imaged in 25 cross sections using a 15° scan, and the INL-INL gap was measured and averaged from the three widest points (shown in *white*). (H) Mean maximal inter-INL width, as determined from naïve (*white bar*; seven eyes), vehicle-treated (*black bar*; 12 eyes), and trabodenoson-treated (*hatched bar*; 13 eyes) animals. Mean interval in micrometers ± SEM. *Double asterisks*: $P < 0.05$. *Triple asterisks*: $P < 0.00001$

In Vivo Electrophysiology

Ganzfeld ERGs were recorded bilaterally using a visual electrophysiology system (UTAS; LKC Technologies, Inc., Gaithersburg, MD). Measurements were obtained at baseline and at 4 weeks post induction. Monopolar rat contact lens electrodes (LKC Technologies, Inc.) were referenced to a silver wire inserted in the mouth, and a skin electrode was affixed to the tail using electrode paste (Grass EC2; Natus Mfg. Ltd, Galway, Ireland). Dark adapted (>8 hours) animals were anesthetized with a mixture of ketamine/xylazine (80 mg/4 mg/kg), and eyes were dilated using 1% tropicamide and topically anesthetized using 0.5% proparacaine. Data were analyzed using Wilcoxon rank sum test because the b-wave data were not normally distributed.

Euthanasia and Tissue Preparation

Following terminal electrophysiological recording, animals were euthanized and eyes enucleated with an attached ON. Eyes were immediately postfixed overnight with ice cold 4% paraformaldehyde-PBS (PF-PBS), pH 7.4. Animals used for ultrastructure were anesthetized to the deep surgical plane, exsanguinated, and then terminally perfused with 2% PF-PBS, followed by postfixation in buffered glutaraldehyde-PF in PBS. Eyes used for RNA isolation were rapidly isolated following euthanasia without fixation, and the retinae were extruded from the globe and frozen on dry ice. The ONH with 0.5 mm of attached ON was dissected from the globe and flash-frozen on ice. Tissues were stored at −80°C until RNA isolation.

RGC Layer Stereology

PF-PBS–fixed retinae were isolated, and RGCs were immunostained and stereologically counted as previously described[28] using a fluorescent microscope (Nikon Eclipse E800; Nikon, Melville, NY) with motorized stage, driven by a stereological imaging package (Stereo Investigator, Ver. 10.0; MBF Bioscience, Williston, VT). Stereological analysis was performed using the Stereo Investigator 10 package,

Table 1. List of Antibodies, Functions, Dilution Conditions

Antibody	Function	Supplier	RRID	Dilution
SMI312	Intact axons	Abcam (mouse)	AB_448151	1:5,000
IBA1	All inflammatory cells	Wako (rabbit)	AB_839504	1:500
GFAP	New GFAP expression	DAKO (rabbit)	AB_10013382	1:10,000
A_1R	A_1 Adenosine receptors	Abcam (rabbit)	AB_2049141	1:1,000
C3d	Inflammation	R&D Systems (goat)	AF2655	1:2,000
Nestin	Neuroprotection	EMD-Millipore (mouse)	AB_2251134	1:1,000
Brn3a	RGC nuclei	Santa Cruz (goat)	AB_2167511	1:500

RRID, Research Resource Identifiers.

with counts in each eye greater than that required by the Schmitz-Hof equation for statistical validity.

ON Immunohistochemical Staining

ON and ONH 10-µm longitudinal sections were used for specific analyses. Antibody to the ionized calcium channel protein IBA1 was used for global cellular inflammation. Newly synthesized macrophages/microglia were identified using CD68 (ED1). Intact axonal neurofilaments were evaluated using SMI312 mouse monoclonal antibody cocktail. We also evaluated GFAP, complement factor 3d fragment (C3d), and nestin expression. Antibody information and dilutions are listed in Table 1.

RNA and Quantitative Real-Time Polymerase Chain Reaction (qPCR)

Total RNA isolation and qPCR was performed from the anterior 1-mm ONH sections and 1-mm sections of midpoint ON. Two-step qPCR analysis was performed after sequential purification of total RNA using phenol-guanidinium (RNA-Bee; Tel-Test Labs, Alvin, TX), DNAse digestion, followed by purification with a microkit (RNAeasy; Qiagen, Inc., Valencia, CA). First-strand random-primed cDNA was generated (Superscript III First-Strand Synthesis; Invitrogen, Carlsbad, CA), and individual gene expression was determined using gene-specific primers. Individual gene assay characteristics are shown in Table 2. A ddCT analysis was performed by comparing internal control gene expression (cyclophilin) against test gene expression. Expression results from noninduced, vehicle-treated tissues were set as a baseline of 1.0. Results were compared against noninduced vehicle. We used the Mann-Whitney nonparametric statistical analysis for evaluating statistical significance.

Axonal Ultrastructure

PF-PBS–fixed ON specimens were postfixed in mixed buffered glutaraldehyde-PF solution, shad-

Table 2. List of Gene-Specific Primers and Characteristics

Gene	Accession#	Sequence	Tm (^{0}C)	Length (bp)	Gene name
Ppib	NM_022536	5'-TTCTCCACCTTCCGTACCA-3'	60	93	Cyclophilin B
		5'-CATAACTACAGTCAAGACCTCCTG-3'			
GFAP	NM_017009	5'-GGAGGGCGAAGAAAACCGCATCA-3'	60	152	Glial Fibrillary Acidic Protein
		5'-TGACCTCGCCATCCCGCATCT-3'			
Nes	NM_012987	5'-GGTCCAGAAAGCCAAGAGAAG-3'	60	118	Nestin
		5'-CACCTCAAGATGTCCCTTAGTC-3'			
Adora1	NM_017155	5'-ACAGACCTACTTCCACACCT-3'	60	141	Adenosine A1R receptor
		5'-GTCACCACTGTCTTGTACCG-3'			
HO-1	NM_012580	5'-GCCTTCCTGCTCAACATTG-3'	60	96	Heme Oxygenase-1
		5'-GCGAAGAAACTCTGTCTGTGA-3'			
Mmp2	NM_031054	5'-GTTTATTTGGCGGACAGTGAC-3'	60	130	Matrix Metalloproteinase-2
		5'-GAACACAGCCTTCTCTTCCT-3'			
Thy-1	NM_012673	5'-TACTCTAGCCAACTTCACCAC-3'	60	265	Thymus-1
		5'-AGCAAGACCTCTTCAGCAGA-3'			
Sox2	NM_001109181	5'-CAGGAGTTGTCAAGGCAGAGA-3'	60	133	Sry Box-2
		5'-CTTAAGCCTCGGGCTCCAAA-3'			

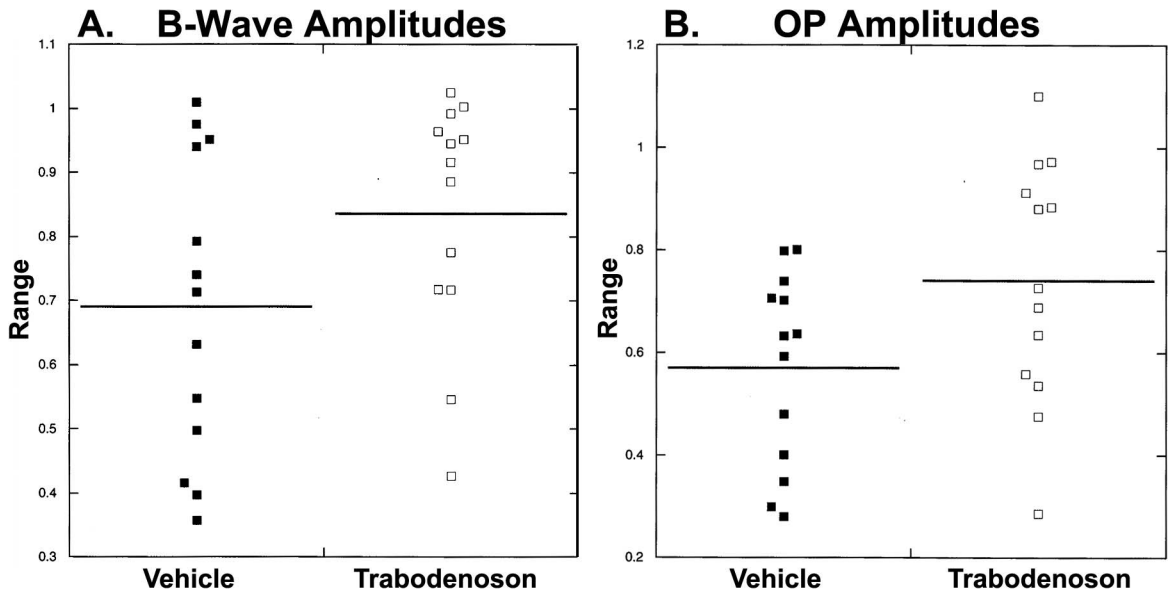

Figure 2. Ganzfeld ERG analysis of vehicle-treated (*black squares*) and trabodenoson-treated (*white squares*) eyes. The ERG ratio (OD/OS) for each animal is shown on the ordinate; the treatment groups are indicated on the abscissa. Mean values are shown as a line. (A) B-wave results. Mean ± 1 SEM for vehicle was 0.69 ± 0.06 vs. 0.84 ± 0.04 for trabodenoson ($P = 0.11$). (B) OP results. Mean ± 1 SEM for vehicle was 0.57 ± 0.05 vs. 0.74 ± 0.07 for trabodenoson ($P = 0.09$). There is a nonsignificant trend toward retinal neuroprotection in trabodenoson-treated animals.

owed with uranyl acetate, embedded in Epon, and cross-sectioned at 200-nm thickness. Cross sections were floated onto copper mesh and examined using an electron microscope (Tecnai FEI T12; FEI, Hillsboro, OR). Images were analyzed at ×2100 and ×4400 magnification.

Results

Trabodenoson Reduces rNAION-Induced ON Edema

Two day postinduction SD-OCT images of the intraocular ON and peripapillary retina were obtained to evaluate the levels of anterior ON edema and peripapillary vascular dilation in vehicle-treated, trabodenoson-treated, and naïve eyes (Fig. 1A,B). ONH edema measurements were taken at seven points, with the three sections exhibiting the widest INL-INL gaps in each eye used for quantification. Mean values (vehicle and trabodenoson treated) were analyzed using ANOVA.

Representative retinal and ONH images are shown in Figure 1A–F; quantification is shown in Figure 1H. Both treatment groups revealed ONH edema (expansion of the INL-INL gap) significantly greater than that compared with not-induced eyes (336.7 ± 25.5 μm SD; $P < 0.00001$; $df = 29$). Comparison of vehicle- and trabodenoson-treated groups also revealed that trabodenoson treatment reduced overall ON edema slightly but significantly compared with vehicle (512.2 ± 72.4 μm [trabodenoson] versus 564.1 ± 49.5 μm [vehicle]; $P < 0.05$).

Trabodenoson May Reduce Ischemia-Induced Retinal Dysfunction

Induction of rNAION, in addition to causing ON ischemia, sometimes will cause central retinal artery and/or vein occlusions leading to inner retinal ischemia. We routinely record ERGs in rNAION animals to identify these animals so that they can be excluded from further study, thus ensuring that damage to the RGCs can be attributed solely to ON ischemia. Interestingly, trabodenoson-treated eyes showed less retinal involvement than did vehicle-treated eyes.

In Figure 2A, B, ERG b-wave amplitudes and oscillatory potentials (OPs) in the induced eye (OD) were normalized to ERG b-wave amplitudes and OPs, respectively, from the contralateral noninduced eye (OS) of the same animal to control for interanimal variation. While the difference in b-wave amplitudes between the vehicle and treated groups was not significant ($P = 0.11$, Wilcoxon), fewer (2/13) of the

trabodenoson-treated animals exhibited significant retinal ischemia (defined as >35% decrease in b-wave ERG amplitude) than did the vehicle-treated animals (6/13). Compared with naïve eyes, vehicle-treated rNAION eyes exhibited a 31% reduction in b-wave amplitude (OD/OS = 0.69 ± 0.06 SEM; $n = 13$), while trabodenoson-treated animals exhibited a 16% reduction (OD/OS = 0.84 ± 0.04 SEM; $n = 13$). OPs were reduced by 43% (0.57 ± 0.05) versus 26% (0.74 ± 0.07) for trabodenoson-treated eyes. This difference was not significant ($P = 0.09$, Wilcoxon). These trends are suggestive of trabodenoson-associated protection against inner retinal ischemia.

Trabodenoson Upregulates ONH-Astrocyte A_1R and Neuroprotection Markers without Reducing Inflammatory Cell Infiltration

Both retinal and ONH-associated A_1R expression was evaluated following early (2 days post induction, 5 days total treatment) in noninduced and induced eyes. There was increased immunological A_1R signal in trabodenoson-treated ONHs in both noninduced and induced eyes (trabodenoson treated, Fig. 3E and M; compare with vehicle treatment, Fig. 3A and I). Quantitative analysis of multiple sections and animals revealed that the trabodenoson-associated increase in immune signal was significant when compared with vehicle-treated specimens ($P = 0.03$ for uninduced and $P = 0.015$ for induced, respectively; Mann-Whitney U-test). ONH-A_1R expression also colocalized with astrocyte-specific *ALDH1L1* (inset, Fig. 3E). This suggested that trabodenoson's neuroprotective effect could be mediated through alterations in ONH-astrocyte function. However, trabodenoson did not significantly increase early ONH protein signal expression of the intermediate filament protein nestin, which has been associated with astrocyte neuroprotective responses,[21,29,30] compared with vehicle-treated eyes (Fig. 3T graph, $n = 3$ animals/group). There was some variation in individual panels (compare Fig. 3D [naïve] and 3H [uninduced-trabodenoson], and Fig. 3L [rNAION-vehicle] and Fig. 3P [rNAION-trabodenoson]).

Similarly, no changes were seen in the reactive astrocyte protein GFAP (generalized astrocyte reactivity) or *ALDH1L1* (cytoplasmic astrocyte marker; data not shown). We also evaluated IBA1 (cellular inflammatory infiltrate) and C3d, an acute inflammatory phase marker polypeptide associated with many inflammatory processes[31] that has recently received interest as a potential marker for activated astrocytes.[32] IBA1 and C3d signals increased to a similar level in both vehicle- and trabodenoson-treated induced ONHs (compare Fig. 3B and 3F [IBA1, noninduced] to Fig. 3J and 3N [induced], and Fig. 3C and 3G [C3d noninduced] to Fig. 3K and 3O [induced]).

Trabodenoson Selectively Upregulates ONH- and Retina-Expressed Genes

qPCR was performed from individual total RNA samples from retina and ONH of vehicle- and trabodenoson-treated eyes ($n = 8$ total with replicates; Table 2). Results are shown in Figure 4. ONH-A_1R expression declined following rNAION induction, but this decline was significant only in vehicle-treated animals. GFAP mRNA expression was not significantly altered in either vehicle- or trabodenoson-treated eyes post rNAION at early times (Fig. 4A; GFAP). Topical trabodenoson significantly upregulated nestin expression in the ONH of induced eyes compared with vehicle-treated no-induced eyes (Fig. 4A ONH: nestin; $P < 0.01$). *Sox2* expression declined significantly only in vehicle-treated eyes post induction, compared with contralateral controls (Fig. 4A, *Sox2*). Heme oxygenase-1 (Hmox1) mRNA levels increased significantly in induced eyes in both trabodenoson- and vehicle-treated eyes, but there was a greater elevation of Hmox1 in trabodenoson-treated induced eyes compared with uninduced vehicle controls (Fig. 4A, Hmox1).

No changes were identifiable in retinal A_1R expression (Fig. 4B, A_1R), while retinal Thy-1 expression (an RGC-expressed gene) was greater in trabodenoson-treated, post rNAION-induced eyes compared with vehicle-treated eyes (Fig. 4B; compare retinal Thy-1 levels before and after induction), consistent with the observation that topical trabodenoson preserves RGCs (see bar graph in Fig. 6G). Mmp-2 expression was greater in trabodenoson-treated eyes compared with vehicle-treated eyes in all groups (Fig. 4B, mmp2). Interestingly, while retinal Hmox1 showed increased expression after rNAION induction in both trabodenoson- and vehicle-treated eyes, Hmox1 expression in trabodenoson-treated eyes was not as elevated compared with vehicle-treated induced eyes ($P < 0.01$), and only vehicle-treated induced eyes revealed a significant increase in Hmox1 compared with contralateral control (Fig. 4B, Hmox1).

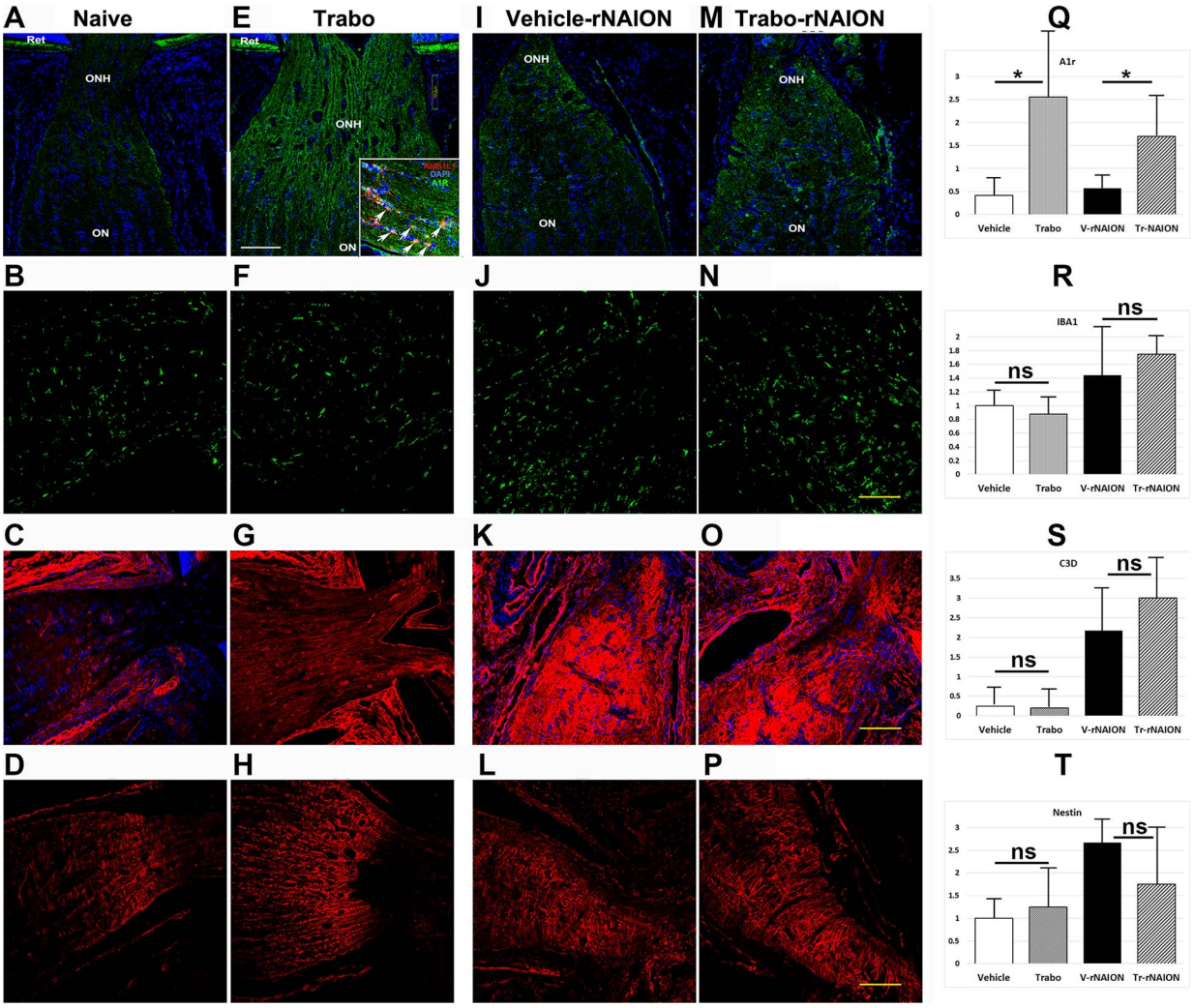

Figure 3. Immunohistochemical analysis of early ONH response to trabodenoson treatment. Treatment is indicated above each column of panels. (A–D) Naïve (vehicle-treated/noninduced) ONH. (E–H) Noninduced/trabodenoson-treated contralateral eye. (I–L) rNAION-induced, vehicle-treated eye (2 days post induction). (M–P) Two days post induction; total 5-day trabodenoson treatment. (Q–T) Mean expression for each protein in percentage of fluorescent intensity (ImageJ software, http://imagej.nih.gov/ij/; provided in the public domain by the National Institutes of Health, Bethesda, MD, USA; $n = 3$ animals). *Top panels*: A_1R receptor expression. ONH and ON A_1R expression colocalized with *ALDH1L1* (*inset*, Fig. 3E), consistent with astrocyte expression of A_1R, but A_1R was also expressed in the ON capillary endothelium (data not shown). Trabodenoson significantly increased A_1R immunoreactivity in uninduced and induced ONHs compared with vehicle treatment (Fig. 3Q). *Second row*: IBA1 expression (total cellular inflammatory infiltrate). Increased IBA1 expression occurs in rNAION-induced eyes of both vehicle- and trabodenoson-treated eyes, with little comparative difference between the two treatment modalities (mean values, Fig. 3R). *Third row*: C3d expression. There is minimal C3d expression in the ONH of noninduced eyes in either vehicle- or trabodenoson-treated ONHs. In contrast, elevated C3d signal is present at similar levels in both treatment groups in rNAION-induced eyes (mean values, Fig. 3S). *Bottom panels*: ONH-nestin immunohistochemical signal in the different treatments (mean values, Fig. 3T). There was no colocalization of C3d with either astrocyte markers GFAP or *ALDH1L1* (data not shown). *Scale bars* in E, N–P: 100 μm.

Trabodenoson Does Not Alter ON Ultrastructure in Surviving Axons Following rNAION

ON-axonal ultrastructure of naïve, vehicle- and trabodenoson-treated ONs is shown (Fig. 5). The naïve ON reveals tightly packed myelinated axons in different nerve regions (center, midperiphery, and peri-sheath) separated by interneural septa (Fig. 5A–C). Few if any degenerate axons are apparent. Thirty days post induction, both vehicle-treated (Fig. 5D–F) and trabodenoson-treated (Fig. 5G–I) eyes show

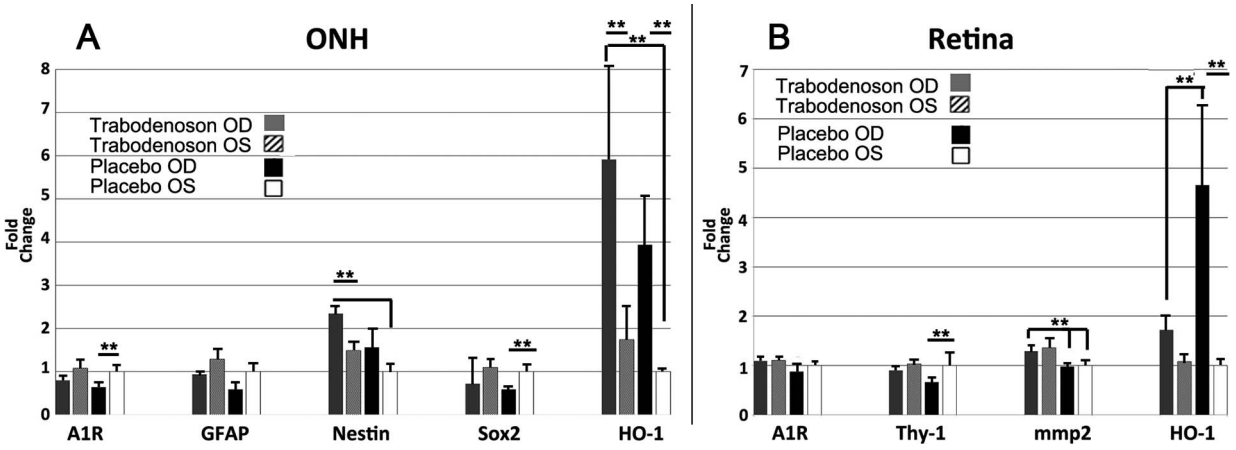

Figure 4. Trabodenoson-associated changes in early ONH and retinal gene expression in noninduced and rNAION-induced eyes. qPCR analysis performed on total RNA from each tissue using gene-specific primer pairs (see Table 2). (A) ONH gene expression. Nestin and Hmox1 increase following induction in both trabodenoson and vehicle-treated eyes. Trabodenoson-treated eyes show increased nestin in the ONH when compared against uninduced placebo ($P < 0.01$), and Hmox1 increases significantly when compared between uninduced and induced tissues in the ONH of both placebo and trabodenoson-treated eyes. *Sox2* expression (neuroprogenitor gene) declined significantly only in vehicle-treated eyes post induction. (B) Retina expression. Retinal Thy-1 declined significantly post rNAION only in vehicle-treated eyes, consistent with RGC neuroprotection. Matrix metalloproteinase (mmp2) gene expression shows a minimal increase after induction in both treatment groups, with higher mmp-2 levels in trabodenoson-treated eyes. Hmox1 expression increased post rNAION in both vehicle and trabodenoson-treated eyes, but vehicle-treated eyes showed a significant increase following induction, compared with Trabodenoson-treated eyes. Comparisons using mean of eight samples per group.

similar ultrastructure (compare different regions in vehicle-treated nerve, Fig. 5D–F, with trabodenoson-treated nerve, Fig. 5G–I). Many degenerate axons were present (double asterisks, Fig. 5D–I) with scattered relative preservation of small-diameter axons in both vehicle- and trabodenoson-treated nerves (Fig. 5D–I, arrows). Relative preservation of small-diameter axons in the rNAION lesion has been previously noted (see Sun et al.[20] Fig. 5). Intact axonal bundles were qualitatively more numerous in ONs from the trabodenoson-treated eyes than in vehicle-treated eyes. Myelin degeneration was similar in both groups.

Trabodenoson Treatment Preserves RGCs Following rNAION

The naïve retina shows rows of Brn3a(+) RGC nuclei (Fig. 6A). Other cells with reduced Brn3a intensity in the RGC layer can be distinguished (Fig. 6A, arrowheads) but are not used in quantification of RGCs. Thirty days post rNAION induction, regional RGC loss occurs in both vehicle- and trabodenoson-treated eyes (Fig. 6B and C; compare with naïve, Fig. 6A). Stereological analysis of Brn3a(+) RGCs post rNAION reveals that vehicle-treated eyes had a mean loss of 53.19% ± 7.08% SEM of their Brn3a(+) RGCs relative to contralateral naïve eyes. In contrast, trabodenoson-treated eyes had a mean loss of 27.87% ± 6.5% SEM Brn3a(+) RGCs relative to noninduced eyes, a statistically significant difference ($P = 0.01$; two-tailed *t*-test). No differences were seen in RGC numbers comparing noninduced eyes across treatment groups (data not shown).

Discussion

We report, to our knowledge, the first identification of a direct neuroprotective effect of a high potency–selective adenosine A_1 mimetic in a preclinical model of ischemic ON damage and identify a likely site of action. Trabodenoson's glaucoma clinical trial determined that this compound did not meaningfully lower IOP compared with other eyedrops (https://clinicaltrials.gov/ct2/show/results/NCT02829996?term=inotek+pharmaceuticals; parts 1–7). However, the study's design combination of short-term total treatment time and reliance on an end point of IOP reduction failed to answer whether trabodenoson could exert RGC-neuroprotective effects via nonocular hypotensive mechanisms; hence, we used the rNAION model, which induces a primary ischemic axonopathy. Thus, this approach may also be relevant to chronic optic neuropathies that have an ischemic component such as OAG.[34–36]

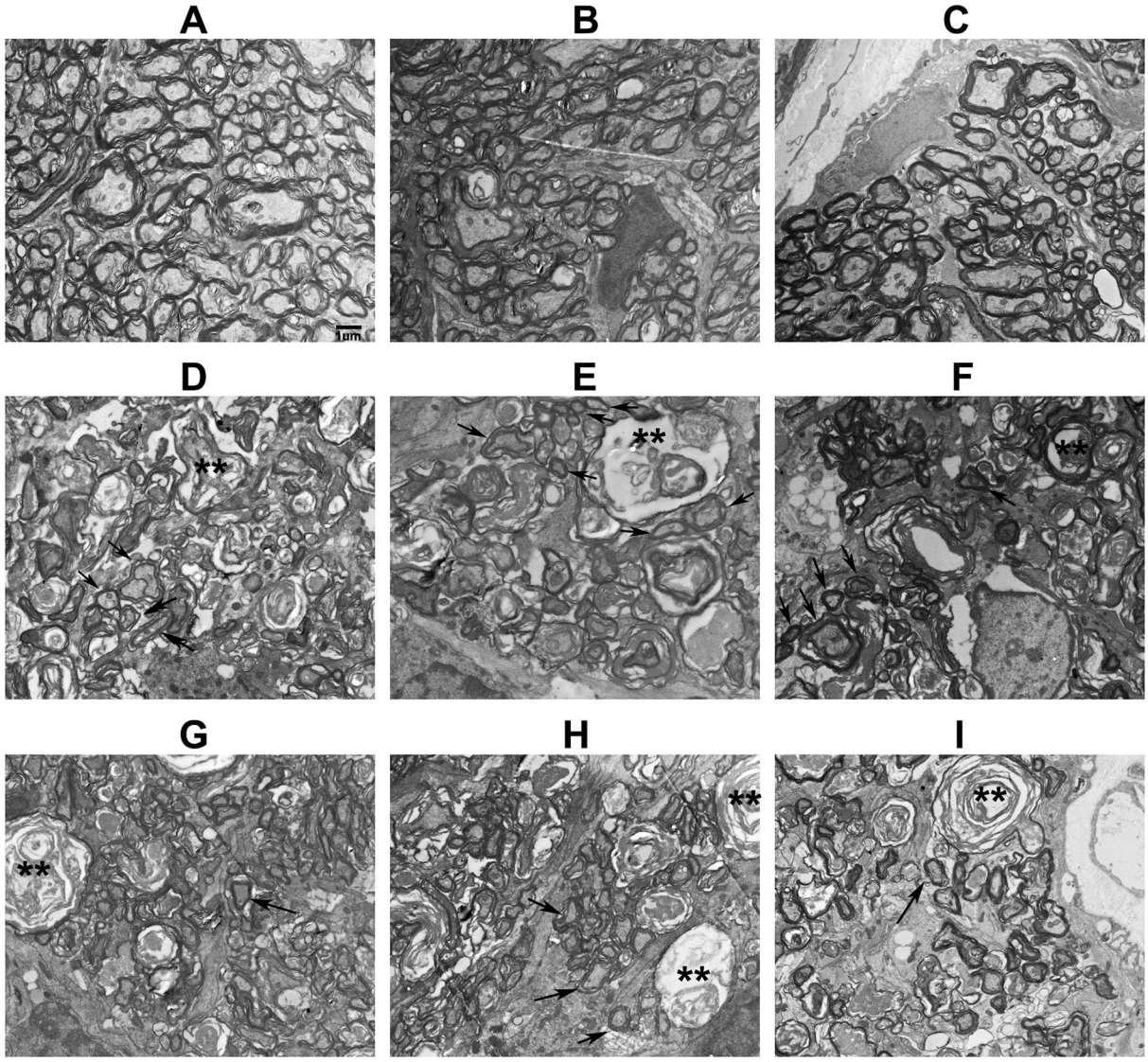

Figure 5. ON ultrastructure evaluated from naïve (A–C); vehicle-treated/induced (D–F); and trabodenoson-induced (G–I) ONs. ONs were at three different regions: central (A, D, G), midperipheral (B, E, H), peripheral (C, F, I). Both trabodenoson- and vehicle-treated eyes showed axonal loss relative to naïve eyes. (A–C) Naïve eyes show closely packed myelinated axons of varying calibers. (D–F) Induced/vehicle treated. Degenerating axons (*double asterisks*) are widely scattered, with adjacent individual and small groups of small caliber, normally myelinated axons (*arrows*). (G–I) Induced/trabodenoson treated. Degenerating axons (*double asterisks*) are present, but there are larger groups of intact axons scattered throughout the ON cross section. There are no apparent differences in degeneration type between vehicle- and trabodenoson-treated eyes (compare E and G). *Scale bar*: 1 μm.

Trabodenoson-treated/rNAION-induced eyes exhibited a modest but statistically significant trend toward ONH edema reduction (compare vehicle and trabodenoson treatment groups in Fig. 1H), suggesting that trabodenoson's neuroprotective site of action was not within the retina, but in the ONH—the site of the primary ischemic lesion. Supporting the ONH as a potential site of A_1R action, we determined that both ONH-A_1R protein and mRNA signals are higher in the corresponding trabodenoson-treated than in vehicle-treated tissues, and this increased expression is significant when compared between rNAION-induced animals. There was no retina A_1R-mRNA–related change for any treatment condition. A_1R agonist RGC-neuroprotective effects may also be mediated via crosstalk with inflammatory mediators such as IL6[5,37] and damage suppression following astrocyte ischemia.[6,38]

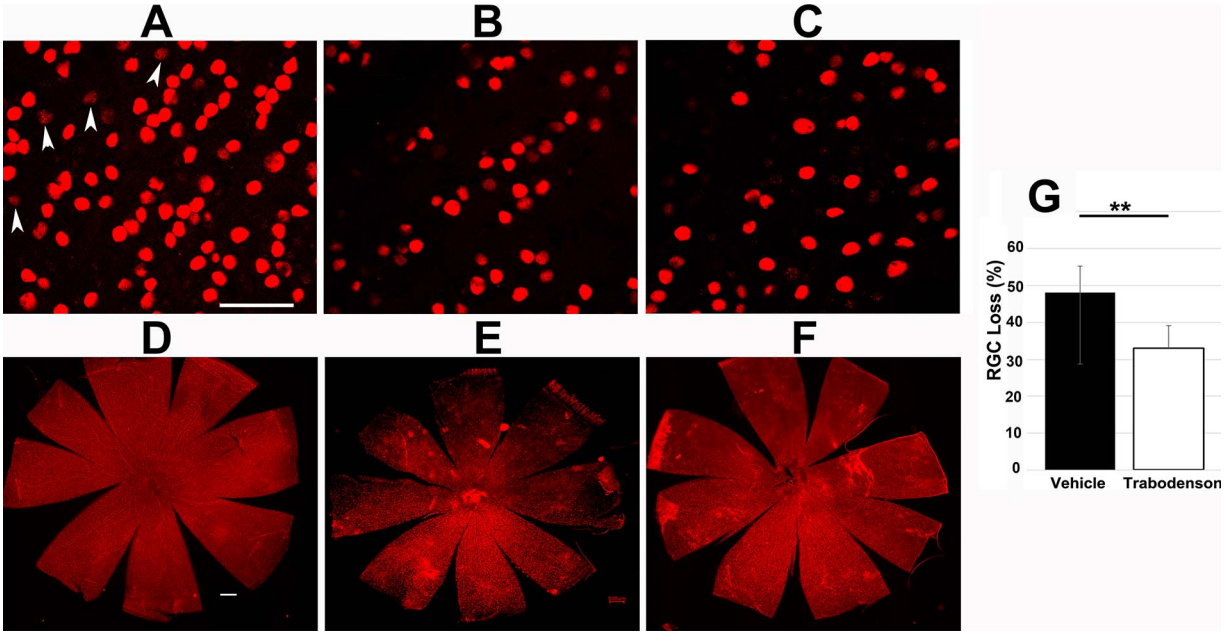

Figure 6. Trabodenoson treatment is neuroprotective to rNAION-induced RGCs. (A–C) Brn3a(+)-stained high-power micrograph immunohistochemical evaluation of retinal flat-mount images from the midperipheral regions. (D–F) Flat-mounted, low-power Brn3a(+) immunostained whole retinal micrographs. (A) Naïve (noninduced) retina. Brn3a(+) strongly reacts with RGC nuclei and weakly, if at all, with other cell nuclei in the RGC layer (*arrowheads*). Many RGC nuclei are associated with the inner retinal vasculature and are linearly arranged. (B) rNAION-induced, vehicle-treated retina. There is a regional loss of many RGC nuclei, which is regionally associated (regional loss data not shown; see similar pattern in Fig. 5B and C in Ulfig, Nikel, and Bohl[33]). (C) rNAION-induced, trabodenoson-treated retina. There are more remaining Brn3a(+) nuclei in all regions of induced retinae. *Scale bar* for 60× images: 100 μm. (D) Naïve (noninduced) retina. (E) rNAION-induced, vehicle-treated retina. (F) rNAION-induced, trabodenoson-treated retina. *Scale bar* in D: 500 μm. (G) RGC-stereological analysis of Brn3a(+) nuclei in flat-mounted retinae from vehicle (*black bars*) and trabodenoson-treated (*white bars*), compared with contralateral noninduced eyes from the each animal. There is statistically significant preservation of RGCs in the rNAION-induced eyes from trabodenoson-treated animals compared with vehicle treatment ($P = 0.01$; two-tailed *t*-test).

Although this study was not powered to examine the drug's effect on inner retinal function, electroretinographic analyses suggested a trend toward retinal neuroprotection by trabodenoson.

A_1R agonists have been associated with a neuroprotective ischemic preconditioning response.[39–41] Hmox1 upregulation is also associated with the ischemic preconditioning response.[42] ONH Hmox1 gene expression increased following topical trabodenoson administration in both the noninduced and rNAION-treated eyes, compared with vehicle-treated eyes. The retinal expression pattern was different from that seen in the ONH: The greatest increase in retinal Hmox1 mRNA was found in induced, vehicle-treated eyes. The upregulation of genes associated with astrocytic neuroprotective responses (such as nestin), without alteration in overall inflammatory infiltration, again suggests that topically administered trabodenoson's neuroprotective effects may be exerted through a combination of retina- and ONH-based activities. Further investigation of trabodenoson's effects at both sites using gene expression and protein-based detection may help to identify other potential pathways associated with A_1-mediated protection.

Trabodenoson-associated axonal preservation was evident at both the immunohistochemical and ultrastructural levels, but there was no difference in the degree of ONH inflammation in vehicle or trabodenoson treatment using Iba1 immunohistochemistry at either early or late postinduction times (see Fig. 3). This suggests that despite reported immunosuppressive effects in transgenic mice in cerebral ischemia,[5] trabodenoson does not generally suppress long-term inflammatory cell invasion of the rNAION lesion. The increased ONH-C3d activity seen post rNAION may be due to breakdown and leakage of the blood–brain barrier, since there was little signal of this complement factor fragment prior to rNAION induction. Further investigation is warranted to determine whether there is a selective alteration of the cellular immune response.

The crucial test of any neuroprotective compound is whether it preserves target neurons. Trabodenoson was strongly neuroprotective in the current trial (vehicle RGC loss, 53.19% ± 7.08% versus trabodenoson treated, 27.87% ± 6.5%, SEM; $P = 0.01$; two-tailed *t*-test; see Fig. 6), supporting our conclusion that the trends toward preservation of retinal function by trabodenoson are real. Additionally, all previously identified NAION and NAION-model neuroprotective compounds have been administered either systemically or intravitreally.[28,43–45] In the current study, trabodenoson was administered topically and still exerted a robust RGC-neuroprotective effect. Our results are consistent with previous reports identifying a direct A_1R agonist neuroprotective effect in models of CNS trauma,[5] CNS ischemic lesions,[38] and otological damage.[46]

An important caveat for the current study is that trabodenoson was administered as a chronic treatment, with administration beginning 2 to 3 days prior to rNAION induction. Thus, it is unclear whether trabodenoson administration would be equally effective if administered after onset of the acute ON ischemia associated with clinical NAION. Further study is required to answer this question. Given the paucity of effective treatments for NAION and the lack of any OAG drugs that exert a direct neuroprotective effect on RGCs or their axons, the low toxicological profile of trabodenoson topical drop therapy make it an attractive candidate for further focused preclinical studies of treatment for both axonal ischemic diseases such as NAION and OAG, as well as for chronic diseases leading to RGC loss.

Acknowledgments

The authors thank Ru-Ching Shi, PhD, and John Strong, MS, (UMB ultrastructural core) for their superb assistance in the ultrastructural portions of this study.

This study was initiated and partially funded by Inotek Pharmaceuticals. This study was also funded by National Institutes of Health Grant RO1-EY015304 (SLB).

Disclosure: **Y. Guo**, None; **Z. Mehrabian**, None; **M.A. Johnson**, None; **D.S. Albers**, None; **C.C. Rich**, None; **R.A. Baumgartner**, None; **S.L. Bernstein**, Inotek Pharmaceuticals (F)

References

1. Miller NR, Arnold AC. Current concepts in the diagnosis, pathogenesis and management of non-arteritic anterior ischaemic optic neuropathy. *Eye*. 2014;29:65–79.
2. Bernstein SL, Johnson MA, Miller NR. Non-arteritic anterior ischemic optic neuropathy (NAION) and its experimental models. *Prog Retin Eye Res*. 2011;30:167–187.
3. Duarte JMN, Cunha RA, Carvalho RA. Adenosine A1 receptors control the metabolic recovery after hypoxia in rat hippocampal slices. *J. Neurochem*. 2016;136:947–957.
4. Arrigoni E, Crocker AJ, Saper CB, Greene RW, Scammell TE. Deletion of presynaptic adenosine A1 receptors impairs the recovery of synaptic transmission after hypoxia. *Neuroscience*. 2005; 132:575–580.
5. Haselkorn ML, Shellington DK, Jackson EK, et al. Adenosine A1 receptor activation as a brake on the microglial response after experimental traumatic brain injury in mice. *J Neurotrauma*. 2010;27:901–910.
6. Ghiardi GJ, Gidday JM, Roth S. The purine nucleoside adenosine in retinal ischemia-reperfusion injury. *Vision Res*. 1999;39:2519–2535.
7. Stockwell J, Jakova E, Cayabyab FS. Adenosine A1 and A2A receptors in the brain: current research and their role in neurodegeneration. *Molecules*. 2017;22:676–694.
8. Li B, Roth S. Retinal ischemic preconditioning in the rat: requirement for adenosine and repetitive induction. *Invest Ophthalmol Vis Sci*. 1999;40: 1200–1216.
9. Haydon PG, Carmignoto G. Astrocyte control of synaptic transmission and neurovascular coupling. *Physiol Rev*. 2006;86:1009–1031.
10. Gessi S, Merighi S, Stefanelli A, Fazzi D, Varani K, Borea PA. A(1) and A(3) adenosine receptors inhibit LPS-induced hypoxia-inducible factor-1 accumulation in murine astrocytes. *Pharmacol Res*. 2013;76:157–170.
11. Migita H, Kominami K, Higashida M, et al. Activation of adenosine A1 receptor-induced neural stem cell proliferation via MEK/ERK and Akt signaling pathways. *J Neurosci Res*. 2008;86:2820–2828.
12. Guo Y, Johnson M, Mehrabian Z, et al. Dendrimers target the ischemic lesion in rodent and primate models of nonarteritic anterior ischemic optic neuropathy. *PLoS One*. 2016;11: e0154437.

13. Sun D, Moore S, Jakobs TC. Optic nerve astrocyte reactivity protects function in experimental glaucoma and other nerve injuries. *J Exp Med*. 2017;214:1411–1430.
14. Bosco A, Breen KT, Anderson SR, Steele MR, Calkins DJ, Vetter ML. Glial coverage in the optic nerve expands in proportion to optic axon loss in chronic mouse glaucoma. *Exp Eye Res*. 2016;150:34–43.
15. Myers JS, Sall KN, Du Biner H, et al. A dose-escalation study to evaluate the safety, tolerability, pharmacokinetics, and efficacy of 2 and 4 weeks of twice-daily ocular trabodenoson in adults with ocular hypertension or primary open-angle glaucoma. *J Ocul Pharmacol Ther*. 2016;32:555–562.
16. Li G, Torrejon KY, Unser AM, et al. Trabodenoson, an adenosine mimetic with A1 receptor selectivity lowers intraocular pressure by increasing conventional outflow facility in mice. *Invest Ophthalmol Vis Sci*. 2018;59:383–392.
17. Rich CC, Albers DS, Gow JA, Baumgartner RA. Targeting the adenosine A1 receptor in the eye with trabodenoson, an adenosine mimetic. In: Samples JR, Knepper P, editors. *Glaucoma Research and Clinical Advances*: *2018 to 2020*. New Concepts in Glaucoma. Vol. 2. Amsterdam: Kugler Publications; 2018:241–258.
18. Lin TN, Cheung WM, Wu JS, et al. 15d-prostaglandin J2 protects brain from ischemia-reperfusion injury. *Arterioscler Thromb Vasc Biol*. 2006;26:481–487.
19. Lee TS, Tsai HL, Chau LY. Induction of heme oxygenase-1 expression in murine macrophages is essential for the anti-inflammatory effect of low dose 15-deoxy-Delta 12,14-prostaglandin J2. *J Biol Chem*. 2003;278:19325–19330.
20. Sun JQ, Cao YT, Liu HQ, Deng WA. Neuroprotective effects of exogenous basic fibroblast growth factor on the hypoxic-ischemic brain damage of neonatal rats. *Zhonghua Er Ke Za Zhi*. 2007;45:354–359.
21. Kuo LT, Groves MJ, Scaravilli F, Sugden D, An SF. Neurotrophin-3 administration alters neurotrophin, neurotrophin receptor and nestin mRNA expression in rat dorsal root ganglia following axotomy. *Neuroscience*. 2007;147:491–507.
22. Agapova OA, Kaufman PL, Lucarelli MJ, Gabelt BT, Hernandez MR. Differential expression of matrix metalloproteinases in monkey eyes with experimental glaucoma or optic nerve transection. *Brain Res*. 2003;967:132–143.
23. Anderson MA, Burda JE, Ren Y, et al. Astrocyte scar formation aids central nervous system axon regeneration. *Nature*. 2016;532:195–200.
24. Balaratnasingam C, Morgan WH, Bass L, et al. Elevated pressure induced astrocyte damage in the optic nerve. *Brain Res*. 2008;1244:142–154.
25. Lojewski X, Hermann A, Wegner F, et al. Human adult white matter progenitor cells are multipotent neuroprogenitors similar to adult hippocampal progenitors. *Stem Cells Transl Med*. 2014;3:458–469.
26. Huang W, Fileta J, Guo Y, Grosskreutz CL. Downregulation of Thy1 in retinal ganglion cells in experimental glaucoma. *Curr Eye Res*. 2006;31:265–271.
27. Bernstein SL, Guo Y, Kelman SE, Flower RW, Johnson MA. Functional and cellular responses in a novel rodent model of anterior ischemic optic neuropathy. *Invest Ophthalmol Vis Sci*. 2003;44:4153–4162.
28. Nicholson JD, Puche AC, Guo Y, Weinreich D, Slater BJ, Bernstein SL. PGJ2 provides prolonged CNS stroke protection by reducing white matter edema. *PLoS One*. 2012;7:e50021.
29. Chen LW, Hu HJ, Liu HL, Yung KK, Chan YS. Identification of brain-derived neurotrophic factor in nestin-expressing astroglial cells in the neostriatum of 1-methyl-4-phenyl-1,2,3,6-tetrahydropyridine-treated mice. *Neuroscience*. 2004;126:941–953.
30. Nakamura T, Xi G, Hua Y, Hoff JT, Keep RF. Nestin expression after experimental intracerebral hemorrhage. *Brain Res*. 2003;981:108–117.
31. Nagar B, Jones RG, Diefenbach RJ, Isenman DE, Rini JM. X-ray crystal structure of C3d: a C3 fragment and ligand for complement receptor 2. *Science*. 1998;280:1277–1281.
32. Liddelow SA, Guttenplan KA, Clarke LE, et al. Neurotoxic reactive astrocytes are induced by activated microglia. *Nature*. 2017;541:481–487.
33. Ulfig N, Nickel J, Bohl J. Monoclonal antibodies SMI 311 and SMI 312 as tools to investigate the maturation of nerve cells and axonal patterns in human fetal brain. *Cell Tissue Res*. 2011;291:433–443.
34. Mehrabian Z, Guo Y, Weinreich D, Bernstein SL. Oligodendrocyte death, neuroinflammation, and the effects of minocycline in a rodent model of nonarteritic anterior ischemic optic neuropathy (rNAION). *Mol Vis*. 2017;23:963–976.
35. Levin LA. Direct and indirect approaches to neuroprotective therapy of glaucomatous optic neuropathy. *Surv Ophthalmol*. 1999;43(suppl 1):S98–101.

36. Cioffi GA. Ischemic model of optic nerve injury. *Trans Am Ophthalmol Soc*. 2005;103:592–613.
37. Howell GR, Soto I, Libby RT, John SWM. Intrinsic axonal degeneration pathways are critical for glaucomatous damage. *Exp Neurol*. 2013; 246:54–61.
38. Perigolo-Vicente R, Ritt K, Goncalves-de-Albuquerque CF, Castro-Faria-Neto HC, Paes-de-Carvalho R, Giestal-de-Araujo E. IL-6, A1 and A2aR: a crosstalk that modulates BDNF and induces neuroprotection. *Biochem Biophys Res Commun*. 2014;449:477–482.
39. Castillo A, Tolon MR, Fernandez-Ruiz J, Romero J, Martinez-Orgado J. The neuroprotective effect of cannabidiol in an in vitro model of newborn hypoxic-ischemic brain damage in mice is mediated by CB(2) and adenosine receptors. *Neurobiol Dis*. 2010;37:434–440.
40. de Jong JW, de Jonge R, Keijzer E, Bradamante S. The role of adenosine in preconditioning. *Pharmacol Ther*. 2000;87:141–149.
41. Hu S, Dong H, Zhang H, et al. Noninvasive limb remote ischemic preconditioning contributes neuroprotective effects via activation of adenosine A1 receptor and redox status after transient focal cerebral ischemia in rats. *Brain Res*. 2012;1459: 81–90.
42. Zeynalov E, Shah ZA, Li RC, Dore S. Heme oxygenase 1 is associated with ischemic preconditioning-induced protection against brain ischemia. *Neurobiol Dis*. 2009;35:264–269.
43. Miller N, Johnson M, Nolan T, Guo Y, Bernstein A, Bernstein S. Sustained neuroprotection from a single intravitreal injection of PGJ2 in a non-human primate model of non-arteritic anterior ischemic optic neuropathy. *Invest Ophthalmol Vis Sci*. 2014;55:7047–7056.
44. Arnold AC, Levin LA. Treatment of ischemic optic neuropathy. *Semin Ophthalmol*. 2002;17:39–46.
45. Huang T-L, Wen Y-T, Chang C-H, Chang S-W, Lin K-H, Tsai R-K. Efficacy of intravitreal injections of triamcinolone acetonide in a rodent model of nonarteritic anterior ischemic optic neuropathy. *Invest Ophthalmol Vis Sci*. 2016;57: 1878–1884.
46. Tabuchi K, Sakai S, Nakayama M, et al. The effects of A1 and A2A adenosine receptor agonists on kainic acid excitotoxicity in the guinea pig cochlea. *Neurosci Lett*. 2012;518:60–63.